Thermo-Mechanical Fatigue Simulation of Exhaust Manifolds

Hojjat Ashouri

Department of Mechanical Engineering, Yadegar-e-Imam Khomeini (RAH) Shahre-Rey Branch, Islamic Azad University, Tehran, Iran

ashouri1394@gmail.com

Abstract

Exhaust manifolds bridge the gap between the cylinder head and the catalytic converter. Loading conditions and complex geometry have led the exhaust manifolds heads to become the most challenging parts of diesel engines. Thermal fatigue failure of the engine components easily happens due to excessive temperature gradient and thermal stress. Modern exhaust systems must withstand severe cyclic mechanical and thermal loads throughout the whole life cycle. This study focuses on the Thermo-mechanical Fatigue (TMF) analysis for exhaust manifolds. During recent years, with the constantly advancing progress of high performance computer technology, many finite element software codes provide the ability to solve finite element analysis coupled problems have been developed. The three-dimensional model of the exhaust manifolds was simulated in abaqus software and a chaboche model was utilized to investigate the elastic and plastic behavior of the exhaust manifolds. This model makes the cyclic stress-strain behavior of the material predictable. The numerical results showed that the temperature and thermal stresses have the most critical values at the confluence region of the exhaust manifolds. This area was under the cyclic tensile and compressive stress and then is under low cycle fatigue. thermo-mechanical fatigue was the main reason for exhaust manifolds failure. After several cycles the fatigue cracks will appear in this region. The lifetime of this part can be determined through finite element analysis instead of experimental tests. Computer aided engineering (CAE) plays an important role to find the weakness of an exhaust manifold layout at the early stage of the engine development.

Keywords: thermo-mechanical fatigue, finite element analysis, exhaust manifolds and confluence cracks

1- Introduction

The exhausts manifolds are mounted on the cylinder head of an engine collects gases exhausted from an engine, and send it to a catalyst converter [1, 2, 3]. They play an important role in the performance of an engine system [1, 4].

Automotive engine works under thermo-mechanical loading conditions. Working temperature increases up to 1000ºC from ambient temperature and thermal stress is prompted by temperature gradient. The temperature difference, which is the result of turning the engine on and off, begets TMF loads on the exhaust manifolds. This thermo-mechanical stresses is one of basic issues in automotive designing will lead to thermo-mechanical failure. The larger temperature variation causes a larger

thermal stress on the structure. Due to cyclic thermal loads, thermo-mechanical fatigue cracks on exhaust manifolds are often observed during engine durability tests, such as thermal shock test. Therefore, selection of materials is of paramount importance since they must have sufficient mechanical strength at high temperatures to be able to withstand cyclic stresses caused by heat [2, 5, 6].

High durability standards, low emissions, minimized vibration and heat dissipation during cold-starting, maximized heat dissipation in high temperature conditions to minimize catalyst ageing and minimizing mass in order to improve fuel economy are among the restrictions making the design of exhaust manifolds a complicated task. Thus, detailed analysis and design are essential [2, 4, 7]. Due to complicated boundary conditions, there is the probability of plastic strain and the creation and growth of fatigue cracks in the exhaust manifolds. Therefore, this simulation and analysis of fatigue cracks in the design of exhaust manifolds is of paramount importance [3].

To prevent fatigue failures, the material selection and the structure evaluation under loads play important role on the design of exhaust manifolds. Concerning material properties, the main characteristics required for the manifold material include good thermal fatigue strength and high oxidation resistance. Hence, ferrous alloys are predominantly employed in the manufacturing of exhaust manifolds. In the present days, exhaust manifolds are manufactured mainly with cast iron and stainless steel. Silicon-Molybdenum is a casting alloy which has extensive use in the automotive industry, especially in exhaust manifolds [8, 9]. By increasing

Silicon and Molybdenum, the cast alloys increases the heat properties, ductility, yield and tensile strength, thermal fatigue life and creep resistance [9, 10]. Delprete et al., have investigated the addition of Silicon, Molybdenum and Chromium on ferritic ductile iron [11].

The exhaust manifold must be capable of operating correctly in different engine conditions which have the highest smoke temperature. As a result, the main determinant factor in choosing the material of exhaust manifold is the maximum smoke temperature. The material used in the exhaust manifold must have the required fatigue strength in high temperatures in order to avoid any wrapping, cracking or leakage related to thermal stresses. For engines with a smoke temperature of less than 244 °C ferritic high silicon cast iron is used, for diesel engines and motors with a smoke temperature of less than 1000°C molybdenum silicon cast iron is applied and for engines with a temperature of more than 1000°C high nickel cast iron is used [12].

Numerous papers have been presented on analysis of stress and fatigue in exhaust manifolds. Partoaa et al. investigated the effect of Effect of fin attachment on thermal stress reduction of exhaust manifolds. Their researches proved that the combined modifications, i.e. the thickness increase and the fins attachments, decrease the thermal stresses by up to 28% and the contribution of the fin attachment in this reduction was much higher compared to the shell thickness increase [13]. Low and high cycle fatigue life estimation of a turbocharged diesel engine exhaust manifolds was studied by Sissa and colleagues. Their research revealed that

vibrational loadings cannot be neglected for correctly estimating the fatigue life of the turbocharged diesel engine exhaust manifolds [4]. Thermo-structure simulation of tractor exhaust manifolds were carried out by Ahmad et al. Their analysis showed that stresses which are produced during the operations for 321-Austenitic Stainless steel exhaust manifold are in the safe region. Thermo-mechanical fatigue was the main reason for exhaust manifolds failure [14].

A combustion and emission characteristic of DI diesel engine fuelled by ethanol injected into the exhaust manifolds was conducted by Nour et al. An ethanol and diesel fuel blending ratio of 15% by volume reported as optimum with regards to performance and emissions. These ethanol and diesel fuel blends increased brake thermal efficiency, CO, and HC emissions while reducing soot and NOx emissions [15]. Szmytka et al. did Thermo-mechanical fatigue of exhaust manifolds. The maximum stress, the same as maximum temperature, occurred in the upper zone of the structure near the turbocharger flange and in the manifold inner skin [16]. Benoit et al. predicted fatigue life of exhaust manifolds by finite element simulation via the energy model of damage. Confluence region was crucial area. The first fatigue cracks can be seen in this area [17]. Thermo-mechanical simulation of manifolds was studied by Mashayekhi et al. The maximum temperature uniformly occurred in the manifold tubes, where the high temperature gas flows in a short thin-walled passage very fast. It can be seen that both the stress and plastic strain, which have the dominant effect on the damage evolution are maximum at the junctions (critical areas) where the expansion of the tubes is restricted by flanges and the cylinder head [18].

Salehnejad et al. established the finite element method and critical fracture toughness for the failure analysis of an exhaust manifold. Their research refuted the possibility of failure in all spots [19]. A cyclic variation of exhaust flows of exhaust manifolds was conducted by Mahabadipour et al. Their research showed the maximum exhaust pressures increased at higher engine load. Also, with increasing the boost pressure, maximum exhaust pressures increased and occurred at more retarded crank angles during the exhaust process [20]. Effects of an exhaust manifold with different structures on the sound order distribution of exhaust noise based on the one-dimensional plane wave theory did by Qiu et al. The isometric exhaust manifold and symmetric isometric exhaust manifolds can control the sound order distribution of the exhaust noise, and they are applicable for improving the sound quality in the future [21].

Santacreu et al. used chaboche model to investigate the elastic, plastic and viscous behavior of the exhaust manifolds. Their research uncovered the fact that viscous strain is significant and its amount is not negligible [2]. Thermo-mechanical analysis of exhaust manifolds of a turbocharged gasoline engine was performed by Chen et al. The simulated results indicate that predicted crack locations and leak area are in agreement with that from the engine durability test [5].

Zhein et al. analyzed unsteady heat transfer of exhaust manifolds. Their research showed a good agreement between strong and serial coupling method results [6].

Coupled CFD-FEA analysis of 6-cylinder diesel engine exhaust manifolds was studied by Vyas et al. A good agreement between experimental and simulated results of the temperature distribution was proved [22]. El-Sharkawy et al. investigated transient thermal analysis of exhaust manifolds. According to their study the experimental and simulated results of temperature match [23].

Thermo-mechanical fatigue of diesel engine exhaust manifolds was examined by Azevedo Cardoso and Claudio Andreatta. Their research refuted the possibility of failure in all spots [9]. Castro Güiza et al. did thermal fatigue fracture of exhaust manifolds. Their analysis indicated that some regions of the cylinder heads entered into yield region. Hence, fatigue cracks appear in them [24]. In another attempt, Low/high cycle fatigue and thermo-mechanical fatigue of exhaust manifolds were examined by Li et al. A good correlation between experimental and simulated results was shown [7].

Ekström et al. investigated the effects of thermal barrier coatings (TBCs) on temperature distribution in the exhaust manifold of a diesel engine. Their research uncovered the fact that thermal barrier coatings reduce the temperature distribution in the substrate of the exhaust manifold about 219°F [25].

According to the introduction, due to the lack of information on the behavior of hardening, softening and viscosity of materials the analysis of exhaust manifolds is mostly based on simple models of material behavior like elastic-plastic and the effects of viscosity and creep of exhaust manifolds are less taken into consideration. The main objective of this study was to simulate the thermo-

mechanical behavior of exhaust manifolds based on the Chaboche model. This model makes the cyclic stress-strain behavior of the material predictable with reasonable accuracy. The model is the best to examine the response of materials such cast iron exhaust manifolds which have remarkable dependent behavior on temperature and plastic at high temperatures. Chaboche model consists of a non-linear kinematic and isotropic hardening model [2]. In some analyses, it is assumed that temperature changes have no effect on the stress-strain curves and thermo-mechanical analysis of exhaust manifolds is non-coupled. Since changes in temperature influence on stress-strain curves, the thermo-mechanical analysis of exhaust manifolds in this study is coupled. In the thermo-mechanical FE model a temperature-dependent properties is used.

2- The material and its behavioral model

In this study the ductile cast iron alloy of Silicon-Molybdenum-Chromium has been used to simulate the thermo-mechanical behavior. The alloy is known as Si-Mo-Cr ductile cast iron which is applied in exhaust manifolds. The chemical composition of the Si-Mo-Cr ductile cast iron is 4.60 wt.% Si, 0.75 wt.% Mo, 1.18 wt.% Cr, 2.45 wt.% C, 0.24 wt.% Mn, 0.02 wt.% P, 0.01 wt.% S, 0.02 wt.% Ni and 0.03 wt.% Cu [11].

Kinematic hardening has both linear and nonlinear isotropic/kinematic model. The first model can be used with Mises or Hill yield surface while the second one can only be used with the Mises yield surface and it is the most accurate and comprehensive model to examine some issues with cyclic loading including cylinder heads of engines. The kinematic hardening model assumes that the yield

surface, proportional to the value of α, moves as back stress in yield zone but it does not deform [26]. Abaqus software uses ziegler linear model [24] to simulate this model as following equation shows:

$$\dot{\alpha}=C\frac{1}{\sigma^0}(\sigma_{ij}-\alpha_{ij})\dot{\bar{\varepsilon}}^{PL}+\frac{1}{C}\dot{C}\alpha_{ij} \qquad (1)$$

In this model σ^0 remains constant. In other words, σ^0 is always equal to σ_0 remain constant. Nonlinear isotropic/kinematic hardening model includes motion of yield surface proportional to the value of α in stress zone and also changes in the size of yield surface is proportional to the plastic strain. This model has been extracted from Chaboche experience [27, 28]. In order to introduce this model a nonlinear term is added to equation (1) to indicate the size of yield surface [26].

The Abaqus software uses nonlinear isotropic/kinematic hardening model as following equation shows:

$$\dot{\alpha}=C\frac{1}{\sigma^0}(\sigma_{ij}-\alpha_{ij})\dot{\bar{\varepsilon}}^{PL}-\gamma_{ij}\dot{\bar{\varepsilon}}^{PL}+\frac{1}{C}\dot{C}\alpha_{ij} \qquad (2)$$

In order to introduce this model in Abaqus software the isotropic and the kinematics parts are required to be defined separately. In order to define the isotropic part the equation (3) is used [29]:

$$\sigma^0=\sigma_0+Q_\infty(1-exp(b\dot{\bar{\varepsilon}}^{PL})) \qquad (3)$$

The overall back stress is computed from the relation (4) [26]:

$$\alpha=\sum_{K=1}^{N}\alpha_K \qquad (4)$$

Heat transfer in engine exhaust manifolds is governed by three effects: conduction through the metal, convection from the hot exhaust gases, and radiative exchange between different parts of the metal surface [7,30].

Heat transfer by conduction per unit area per unit time, $\dot{q}$, in steady situation is given by Fourier law [30]:

$$\dot{q}=-k\nabla T \qquad (5)$$

Heat loss due to thermal radiation between the manifold surface and environment is modeled by the standard Stefan–Boltzmann relation [30, 31]:

$$\dot{q}=\varepsilon\sigma(T_g^4-T_a^4) \qquad (6)$$

Heat convection from exhaust gas to manifold wall is mainly due to forced convection and is strongly dependent on the gas flow dynamics and the manifold geometry. Chirchil and Chu law is used in order to consider heat convection from manifold surface to ambient air, the equation of which is following [32]:

$$Nu=(0.6+(\frac{0.387Ra^{\frac{1}{6}}}{(1+(\frac{0.599}{Pr})^{\frac{9}{16}})^{\frac{8}{27}}}))^2 \qquad (7)$$

3- The finite element model and material properties

TMF analysis of each component needs the cyclic stress-strain distribution. Hot components of engines had complex geometry and loading, and the applying analytical methods for the detection of stress-strain distribution in them are impossible. Many researchers have used finite element method to obtain stress-strain distribution in of geometrically complex components [33]. The exhaust manifolds assemblage analyzed in this article are shown in Figure.1.

Exhaust manifolds consists of a four tube exhaust manifolds with three flanges, bolted with seven bolts to a small section of the engine head. The manifold is cast from ductile gray iron with a Young's modulus of 178 GPa, a Poisson's ratio of 0.29, and a coefficient of thermal expansion of 12.8×10^{-6} per °C.
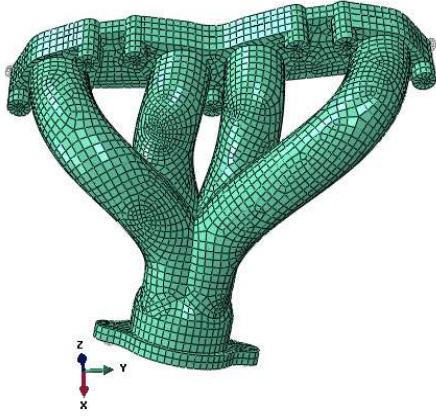
Fig.1. The meshed exhaust manifold [34]

The head is made from aluminum, with a Young's modulus of 69 GPa, a Poisson's ratio of 0.33, and a coefficient of thermal expansion of 22.9×10^{-6} per °C. The head has four exhaust ports leading into the manifold tubes. It has seven bolt holes used to secure the manifold. Seven bolts fasten the manifold to the head. The bolts are made from steel, with a Young's modulus of 207 GPa, a Poisson's ratio of 0.3, and a coefficient of thermal expansion of 13.8×10^{-6} per °C.

All three structural components (manifolds, heads, and bolts) are modeled with three-dimensional continuum elements. The model consists of 7450 first-order brick elements with incompatible deformation modes, C3D8I, and 282 first-order prism elements, C3D6. The C3D6 elements are used only where the complex geometry precludes the use of C3D8I elements. The C3D8I elements are selected to represent the bending of the manifold walls with only one element through the thickness of the tube walls.

exhaust manifolds loading was done in three phases involving apply prescribed bolt loads to fasten the exhaust manifolds to the engine head, subject the assembly to the steady-state operating temperature

distribution and return the assembly to ambient temperature conditions.

4- Result and Discussion
4- 1- Apply prescribed bolt loads

The main loads for thermo-mechanical analysis of exhaust manifolds are the clamping forces introduced by bolts fastening and the material expansion–contraction due to temperature variation during the engine operation [9]. In the first step of the analysis each of the seven bolts is tightened to a uniform bolt force of 20 kN. In subsequent steps the variation of the bolt loads is monitored as the bolts respond to the thermal loading on the assembly as a whole. The prescribed assembly load capability of Abaqus is used. A static analysis procedure is used for this purpose. The maximum principal stress distribution is depicted in Figure 2 proving the stress in the confluence region is tensile. This corresponds to the results by [9, 35].
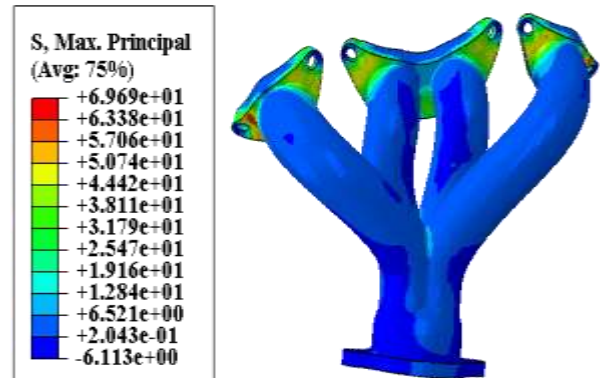
Fig. 2. The maximum principal stress distribution in the first stage of loading

Figure 3 is a plot of the forces carried by each of the seven bolts throughout the load history. The loads carried by the bolts increase significantly during the heat-up step. The loads do not return precisely to the original bolt load specification upon cool down because of the residual stresses,

plastic deformation, and frictional dissipation that developed in the manifolds.
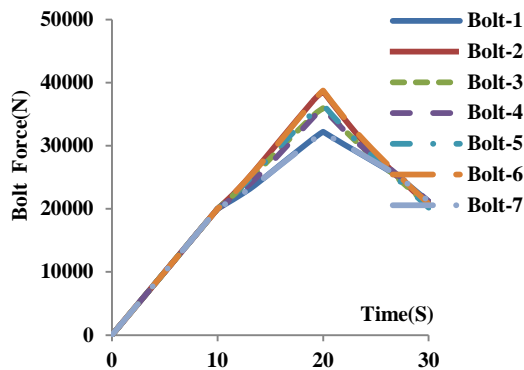
Fig. 3. History of bolt forces

4-2- Thermal Analysis

Thermal analysis includes the simulation of working condition in steady and transient state [31]. In these conditions, exhaust manifolds are subject to thermal exchange phenomena as conduction, convection, radiation [7]. Thermal analysis goal is the evaluation of temperature distribution in exhaust manifolds [2, 5].

Temperature peak and temperature distribution of exhaust manifolds are dominant factors in TMF durability assessment, since the thermal fatigue crack and gasket leakage can be initiated by thermal deformation due to spatial and temporal temperature variations [3,5]. The ability to accurately predict skin temperature for vehicle exhaust system is very important for a robust/durable design of the vehicle exhaust system [1, 6].

Accurate prediction of the temperature of the engine is very crucial and increases the precision of the FEA results. As the accuracy of thermal analysis increases the accuracy of mechanical analysis and fatigue life estimation rises [5, 18].

The manifolds are cast from ductile cast iron with a thermal conductivity of 34

W/mm°C, a density of 7100 kg/m^3, and a specific heat of 460 J/kg°C. The manifolds begin the analysis with an initial temperature of 20°C. The Stefan Boltzmann constant is taken as $5.669*10^{-14}$ W/mm^{2}K^4 and absolute zero is set at 273.15°C below zero. The surface emissivity of ductile cast iron is taken as a constant value of 0.77. For the Si-Mo-Cr ductile cast iron temperature dependent parameter have been provided in order to predict the temperature and stress of the exhaust manifolds.

The hot exhaust gases create a heat flux applied to the interior tube surfaces. In this article this effect is modeled using a surface-based film condition, with a constant temperature of 816°C and a film condition of $500*10^{-6}$ W/mm^2°C. A temperature boundary condition of 355°C is applied at the flange surfaces attached to the cylinder head, and a temperature boundary condition of 122°C is applied at the flange surfaces attached to the exhaust. In this analysis one thermal cycles are applied to obtain a steady-state thermal cycle. Each thermal cycle involves two steps: heating the exhaust manifolds to the maximum operating temperature and cooling it to the minimum operating temperature.

The temperature distribution of exhaust manifolds is shown in Figure 4. Similarly, temperature was high in most regions, especially in the junction of four pipes (confluence region) and the maximum reached 756.9°C. This corresponds to the results by [4]. Temperature peak and temperature distribution of exhaust manifolds are dominant factors in TMF durability assessment, since the thermal fatigue crack can be initiated by thermal

deformation due to spatial and temporal temperature variations.
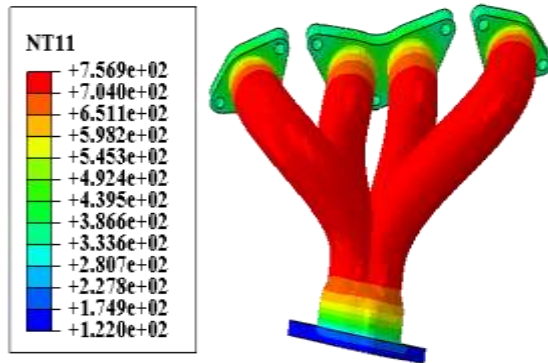
Fig. 4. The temperature distribution in the exhaust manifold

Thermal loading has a considerable effect on the fatigue life and the temperature field identifies critical regions. Crack initiation is due to the changes in the temperature field [5, 9].

4-3- Mechanical Analysis

Engine exhaust manifolds are commonly subject to severe thermal cycles during operation and upon shutdown. Thermal expansion and contraction of the exhaust manifolds is constrained by their interaction with the engine head to which it is bolted. These constraints govern the thermo-mechanical fatigue life of the exhaust manifolds [9, 35].

The cyclic thermal loads are applied in the third analysis step. Nodal temperatures calculated by the previous thermal analysis have been imported in the structural model as thermal loads. It is assumed that the engine head is securely fixed to a stiff and bulky engine block, so the nodes along the base of the head are secured in the direction normal to the base (the global x-direction) but are free to move in the two lateral directions to account for thermal expansion. It is also assumed that the bolts are threaded tightly into the engine head, with the bolt threads beginning directly

beneath the section of engine head modeled. Therefore, the nodes at the bottom of the bolt shanks are shared with the nodes of the surrounding engine head elements and are also secured in the global X direction. The manifold flanges are sandwiched between the top of the engine head and the base of the bolt heads using the *CONTACT PAIR option. The line of action of the bolt forces (bolt shank axes) is along the global x degree of freedom. Soft springs acting in the global Y and Z directions are attached to the outlet end of the manifold and to the two ends of the head to suppress rigid body motions of the manifold and head, respectively. These springs have no influence on the solution.

Von-Mises stress distribution at the end of the third stage is shown in Figure 5. The maximum value of Von-Mises stress in the exhaust manifolds is calculated 487 Mpa. Comparing this result to the yield stress of the exhaust manifolds can be a criterion for the crack initiation. This can leads to the crack initiation. The maximum Von-Mises stress was at the intersection of tubes (confluence area) of the exhaust manifolds, except for the areas around the screws where there was stress concentration.
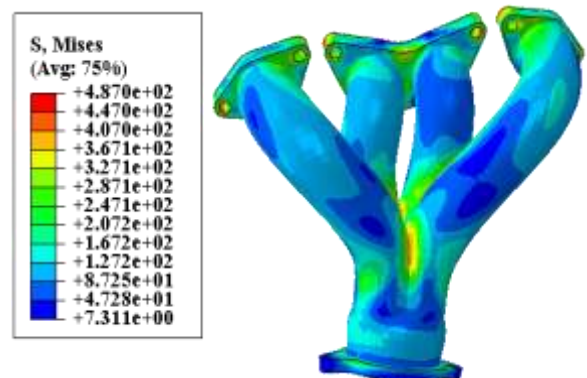
Fig. 5. The Von-Mises stress distribution at the end of the third stage of loading

Based on the source [5] the first fatigue cracks can be seen at the hottest spot of

cylinder heads (Figure 4). This region is also located in the confluence region.

Equivalent plastic strain (PEEQ) distribution is depicted in Figure 6. PEEQ is greater than zero, indicating that the material is currently yielding. PEEQ is specified as part of plasticity behavior definition; the hazardous position can be found where the PEEQ maximum is. As stated in sources [3,8] the initiation of fatigue cracks in exhaust manifolds occurs where plastic strain happens because of thermo-mechanical loads.
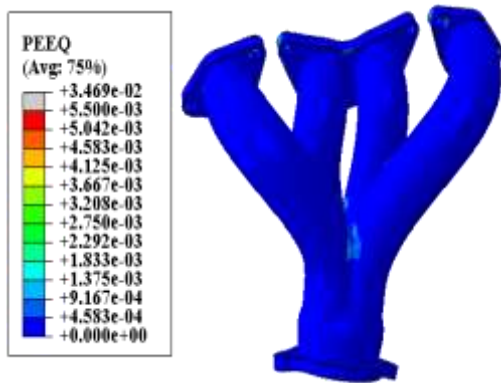
Fig. 6. The equivalent plastic strain distribution

Equivalent plastic strain curve could clearly manifest the PEEQ characteristic of dangerous point that changed with time [6]. It can be seen that both the stress and plastic strain, which have the dominant effect on the damage evolution are maximum at the junctions (critical areas) where the expansion of the tubes is restricted by flanges and the cylinder head.

As presented in Figure 7, the PEEQ rise when the engine is running and it will constant at the end of cycle. As the Figure presents this spot lies in the plastic region when the engine stops. Fatigue damage would prone to happen if the plastic strain accumulated in repeated cycles under the actual operating mode.
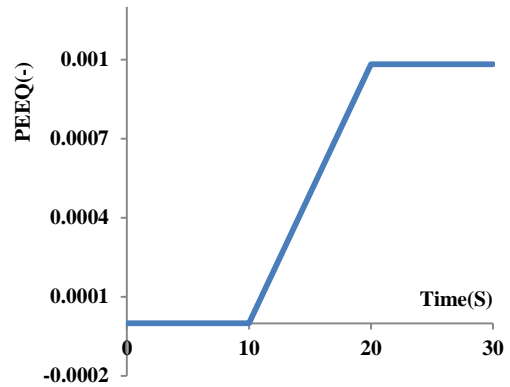
Fig. 7. Equivalent plastic strain curve for the point 1 of element 6674

As shown in Figure 8 some regions of the exhaust manifolds entered into yield zone. As mentioned in the sources [18] these regions are where fatigue cracks initiate. Failures of exhaust manifolds are mainly caused by the extreme temperature gradients the part has to withstand. Cyclic temperature loading causes a few areas to exhibit local cyclic plastic straining of the material, which may cause a crack initiation.
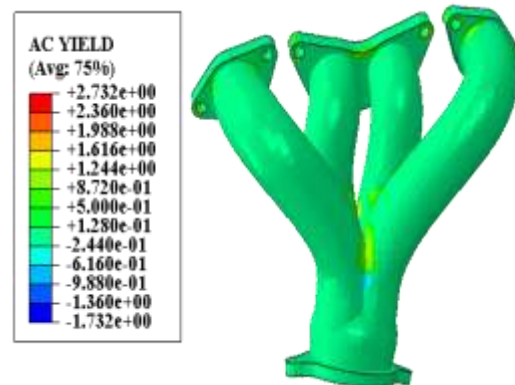
Fig. 8. The regions of exhaust manifold entered into yield zone

Changes of plastic yield for the point 1 of element 6674 are shown in Figure 9. Cyclic plastics yield occurs at this spot for the sake of cyclic loading of exhaust manifolds. The number 1 indicates the existence of plastic yield and the number 0 indicates its non-existence in this region.

According to sources [3, 4, 6] After several cycles of thermal loading, fatigue cracks occur at this spot.
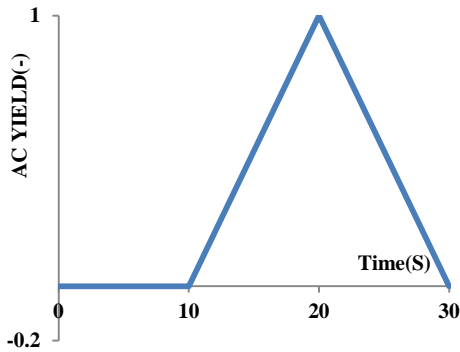
Fig.9. The changes of plastic yield for point 1 of element 6674 versus time

According to the Von-Mises criterion, when the effective stress exceeds the maximum material failure rate rupture occurs. According to Tresca criterion, when the highest shear stress is greater than half of the final failure rate fracture occurs. The distribution of stress in the Von-Mises and Tresca criteria is shown in Figures 5 and 10. The maximum stress in the Von-Mises and Tersca criteria is at the confluence of the exhaust manifold, except for the areas around the screws where there is stress concentrations. According to Figures 5 and 10, the Von-Mises criterion confirms the results of the Tresca criterion.
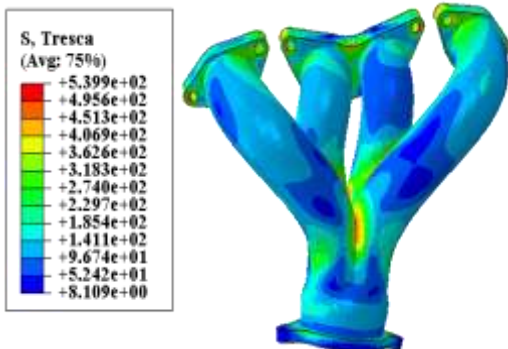
Fig. 10. The Tresca stress distribution at the end of the third stage of loading

Figure 11 displays diagram of normal stresses (S11) in the X direction for point 1

of element 6674. These elements are in the confluence region. Cracking mechanism happens when the engine is running and warm reaching to the highest temperature.. Stresses are compressive because of the thermal loading at the moment (Figure 11, twentieth second). Figure 12 demonstrates vectors of the maximum principal stress in the confluence region when the engine is running. As the Figure represents the maximum principal stress in the confluence is compressive. This corresponds to the results by [18].
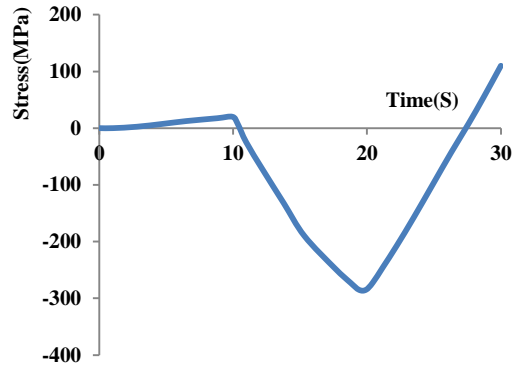
Fig.11. The normal stresses in the X direction for point 1 of element 6674 versus time
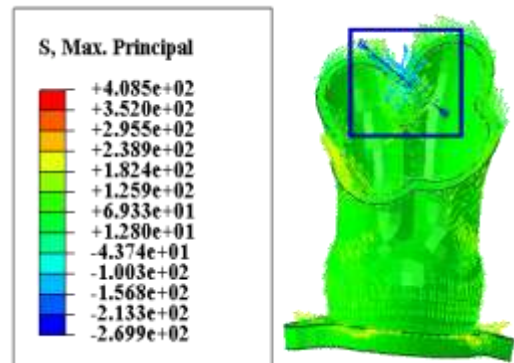
Fig. 12. The maximum principal stress vectors in the confluence when engine running (in twentieth second)

The thermal loading and mechanical constraints generate a compressive stress field, which may drive to compressive yield surface (Figure 9). As the engine shuts off and its temperature gradually

decreases to the room temperature, the stress is tensile for the sake of assembly loads which corresponds to the results of sources [9] (Figure 11, thirtieth second). Figure 13 shows vectors of the maximum principal stress in the confluence when the engine shuts off. As the Figure represents the maximum principal stress in the valves bridge is tensile.
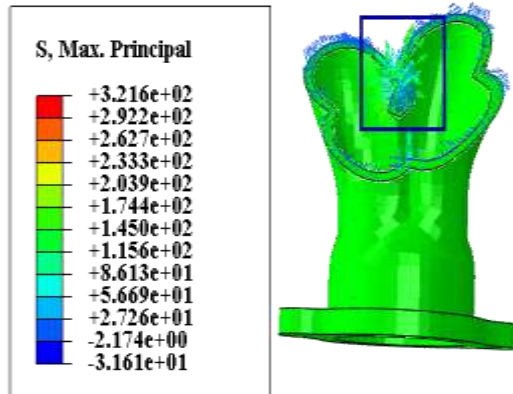
Fig. 13. The maximum principal stress vectors in the confluence when engine shuts off (in thirtieth second)

In the critical area, large compressive plastic deformations are generated in run (hot) condition, and in stop (cold) condition, tensile stresses remain. The cyclic repetition of hot and cold conditions results in a thermal surface cracks which then progressively propagates through the thickness and failure happens. The yielding regions of the exhaust manifolds cannot return to the primary condition. Hence, tensile stress is created in this area and elastic regions. The stress field for the yield surfaces is compressive at high temperature and turns into tensile stress at low temperature; it is correspondence to the results of sources [9,18].The confluence region is under the cyclic tensile and compressive stress which corresponds to the results of sources [1]. According to the source [1, 5, 9] changes in cyclic compressive and tensile stresses cause cracks in exhaust manifolds. As

noted in the source [8] after a several cycles the cast iron ages and drastically loses its strength. Aged material is unable to resist high tensile stresses, then cracks in the exhaust manifolds will appear.

5- Conclusion

In this study coupled thermo-mechanical analysis of exhaust manifolds is studied. A chaboche model is used for this purpose. This model makes the cyclic stress-strain behavior of the material predictable. Finite element analysis provides accurate and reliable prediction of temperature and fatigue results in the exhaust manifolds. The results of the thermo-mechanical analysis indicated that the maximum temperature and stress occurred in the confluence. Investigation of stress distribution in Von-Mises and Tresca criteria of failure showed that confluence of exhaust manifold is a critical area and fatigue cracks originate in this area.

Obtained FEA results proved the stresses in the confluence is compressive when the engine is running and becomes tensile when the engine shuts off. The confluence was under the cyclic tensile and compressive stress, in which the plastic strain happens. Low-cycle fatigue always occurs in this region and fatigue cracks appear after a few cycles. Changes in cyclic compressive and tensile stresses causes cracks in exhaust manifolds. In order to prevent exhaust manifolds cracking it is recommended to modify geometry of material in crucial parts. TBC might also be used in the regions which not only reduce temperature, but also increase the fatigue life of exhaust manifolds. Since they reduce thermal stress, fatigue life of the exhaust manifolds grows. Temperature was effective on stress-strain curves and

thermo-mechanical analysis of the cylinder heads must be coupled.

Nomenclature

C	kinematic hardening modulus
$\dot{C}$	exchange rate of C in temperature
$\dot{\varepsilon}^{PL}$	rate of equivalent plastic strain
σ^0	size of the yield surface
σ_0	yield stress in zero plastic strain
α	back stress
C	material constant
γ	material constant
Q_∞	material constant
b	material constant
$\dot{q}$	heat flux
k	thermal conductivity
∇T	temperature difference
ε	emissivity
σ	standard Stefan–Boltzmann constant
T_a	air temperature
T_g	manifold temperature
Nu	Nusselt number
Ra	Rayleigh number
Nu	Nusselt number
Pr	Prandtl number

References

[1] L. Meda, Y. Shu, and M. Romzek,"Exhaust System Manifold Development," SAE Technical Paper No.2012-01-0643, 2012.

[2] P-O. Santacreu, L. Faivre, and A. Acher, "Life Prediction Approach for Stainless Steel Exhaust Manifold," SAE Technical Paper No.2012-01-0732, 2012.

[3] Z. Yan, L. Zhien, W. Xiaomin, H. Zheng, and Y. Xu, "Cracking failure analysis and optimization on exhaust manifold of engine with CFD-FEA coupling, " SAE Technical Paper No. 2014-01-1710, 2014.

[4] S. Sissaa, M. Giacopinia, and R. Rosia, "Low-Cycle Thermal Fatigue and High-Cycle Vibration Fatigue Life Estimation of a Diesel Engine Exhaust Manifold, " Journal of Procedia Engineering, vol. 74 , 2014, pp. 105-112.

[5] M. Chen, Y. Wang, W. Wu, and J. Xin, "Design of the Exhaust Manifold of a Turbo Charged Gasoline Engine Based on a Transient Thermal Mechanical Analysis Approach," SAE Technical Paper No.2014-01-2882, 2014.

[6] L. Zhien, X. Wang Z. Yan, X. Li, and Y. Xu, "Study on the Unsteady Heat Transfer of Engine Exhaust Manifold Based on the Analysis Method of Serial, " SAE Technical Paper No.2014-01-1711, 2014.

[7] X. Li, W. Wang, X. Zou, Z. Zhang, W. Zhang, S. Zhang, T. Chen, Y. Cao, and Y. Chen, "Simulation and Test Research for Integrated Exhaust Manifold and Hot End Durability," SAE Technical Paper No .2017-01-2432, 2017.

[8] X. Liu, G. Quan, X. Wu, Z. Zhang, and C. Sloss, "Simulation of Thermomechanical Fatigue of Ductile Cast Iron and Lifetime Calculation," SAE Technical Paper No.2015-01-0552, 2015.

[9] A-D. Azevedo Cardoso, and D. Claudio Andreatta, "Thermomechanical Analysis of Diesel Engine Exhaust Manifold," SAE Technical Paper No.2016-36-0258, 2016.

[10] X. Wu, T. Quan, and C. Sloss, "Failure Mechanisms and Damage Model of Ductile Cast Iron under Low-Cycle Fatigue Conditions," SAE No.Technical Paper 2013-01-0391, 2013.

[11] C. Delprete, R. Sesana, "Experimental characterization of a Si–Mo–Cr ductile cast iron," Journal of Materials and Design, vol. 57, 2014, pp. 528-537.

[12] H. Yamagata, The science and technology of materials in automotive engines, Woodhead Publishing Limited Cambridge, UK, 2005.

[13] A.A Partoaa, M. Abdolzadeh, and M. Rezaeizadeh, "Effect of fin attachment on thermal stress reduction of exhaust manifold of an off road diesel engine," DOI: 10.1007/s11771-017-3457-1, 2017, pp. 546-559

[14] F. Ahmad, V. Tomer, A. Kumar, and P.P. Patil, "FEA Simulation Based Thermo-mechanical Analysis of Tractor Exhaust Manifold," Springer India, CAD/CAM, Robotics and Factories of the Future, Lecture Notes in Mechanical Engineering, DOI 10.1007/978-81-322-2740-3-18 , 2016, pp. 173-181.

[15] M. Nour, H. Kosaka, M. Bady, S. Sato, and A.K. Abdel-Rahman, "Combustion and emission characteristics of DI diesel engine fuelled by ethanol injected into the exhaust manifold," Fuel Processing Technology, vol. 164, 2017, pp. 33–50

[16] F. Szmytka, P. Michaud, L. Rémy, and A. Köster, "Thermo-mechanical fatigue resistance characterization and materials ranking from heat-flux-controlled tests. Application to cast-irons for automotive exhaust part," Journal of Fatigue, vol. 55, 2013, pp. 136–146

[17] A. Benoit, M.H. Maitournam, L. Rémy, and Y. Oger, "Cyclic behaviour of structures under thermomechanical loadings: Application to exhaust manifolds," Journal of Fatigue, vol. 38, 2012, pp. 65–74

[18] M. Mashayekhi, A. Taghipour, A. Askari, and M. Farzin, "Continuum damage mechanics application in low-cycle thermal fatigue," International Journal of Damage Mechanics, vol. 22, no.2, 2012. pp. 285-300.

[19] M.A.Salehnejad, A. Mohammadi, M. Rezaei, and H. Ahangari, "Cracking failure analysis of an engine exhaust manifold at high temperatures based on critical fracture toughness and FE simulation approach," Journal of Engineering Fracture Mechanics, DOI.org/10.1016/j.engfracmech.2019.02. 005, 2019, pp. 1-54

[20] H.Mahabadipour, R.S. Krishnan, and K.K. Srinivasan, "Investigation of exhaust flow and exergy fluctuations in a diesel engine," DOI .org/10.1016/j.applthermaleng.2018.10.10 9, Applied Thermal Engineering, 2018, pp. 1-37

[21] S. Qiu, Z.C Yuan, R.X. Fan, and J. Liu, "Effects of exhaust manifold with different structures on sound orderdistribution in exhaust system of four-cylinder engine, " Journal of Applied Acoustics, vol.145, 2019, pp. 176–183

[22] S. Vyas, A. Patidar, S. Kandreegula, and U. Gupta, "Multi-Physics Simulation of 6-Cylinder Diesel Engine Exhaust Manifold for Investigation of Thermo-Mechanical Stresses," SAE Technical Paper No.2015-26-0182, 2015.

[23] A. El-Sharkawy, A. Sami, A. Hekal, D. Arora, and M. Khandaker, "Transient Modeling of Vehicle Exhaust Surface Temperature," SAE No.Technical Paper 2016-01-0280, 2016.

[24] G.M. Castro Güiza, W. Hormaza, R. Andres, E. Galvis, and L.M. Méndez Moreno, "Bending overload and thermal fatigue fractures in a cast exhaust Manifold, " Journal of Engineering Failure Analysis, doi: 10.1016/j.engfailanal.2017.08.016, 2017.

[25] M. Ekström, A. Thibblin, A. Tjernberg, C. Blomqvist, and S. Jonsson, "Evaluation of internal thermal barrier coatings for exhaust manifolds, "Journal of surface & coating technology, vol. 272, 2015, pp. 198-212

[26] J. Lemaitre, and J. Chaboche, Mechanics of Solid Materials, Cambridge University Press, Cambridge, 1990.

[27] J. L. Chaboche, "Time-independent constitutive theories for cyclic plasticity, " International Journal of Plasticity, vol. 2, No. 2**,** 1986, pp. 149–188

[28] J. L. Chaboche, "A review of some plasticity and viscoplasticity constitutive theories," International Journal of Plasticity, vol. 24, 2008, pp. 1642–1693

[29] A. Deshpande, S.B. Leen, and T.H. Hyde, "Experimental and numerical characterization of the cyclic thermo-mechanical behavior of a high temperature forming tool alloy," ASME Journal of Manufacturing Science and Engineering, vol. 132, 2010, pp. 1-12.

[30] J.B. Heywood, Internal combustion engine fundamentals, McGraw-Hill press, 1998.

[31] A.C. Alkidas, P.A. Battiston, and D.J. Kapparos, "Thermal Studies in the Exhaust System of a Diesel-Powered Light-Duty Vehicle," SAE Technical Paper No.2004-01-0050, 2004.

[32] Y. He, P. Battiston, and A. Alkidas, "Thermal Studies in the Exhaust Manifold of a Turbocharged V6 Diesel Engine Operating Under Steady-State Conditions," SAE Technical Paper No.2006-01-0688, 2006.

[33] G.Q. Sun, and D.G Shang, "Prediction Of Fatigue Lifetime Under Multiaxial Cyclic Loading Using Finite Element Analysis," Journal of Material and Design, vol. 31, 2010, pp. 126-133.

[34] ABAQUS/CAE(v6.13-1), User's Manual , 2013.

[35] N. Mamiya, T. Masuda, and Y. Yasushi Noda, 2002, "Thermal Fatigue Life of Exhaust ManifoldsPredicted by Simulation," SAE Technical Paper No.2002-01-0854, 2002.